Organic Electronics 69 (2019) 106–113

Contents lists available at ScienceDirect

Organic Electronics

journal homepage: www.elsevier.com/locate/orgel

Probe-induced resistive switching memory based on organic-inorganic lead halide perovskite materials

Abbas Shaban[a,b], Mojtaba Joodaki[a,b,*], Saeed Mehregan[b], Ivo W. Rangelow[c]

[a] Department of Electrical Engineering, Ferdowsi University of Mashhad, 9177948974, Mashhad, Iran
[b] Organic Nano-Electronic and Organic Solar Cell Lab, Ferdowsi University of Mashhad, 9177948974, Mashhad, Iran
[c] Dept. of Micro- and Nanoel. Syst., Ilmenau University of Technology, 98684, Ilmenau, Germany

ARTICLE INFO

Keywords:
Resistive memory
RRAM
Probe based memory
Perovskite memory
Iodide vacancy
Silver epoxy

ABSTRACT

In this paper we demonstrate a resistive storage device with $CH_3NH_3PbI_{3-x}Cl_x$/FTO structure which stores information in two levels of resistance states induced by electrical probe excitation. The perovskite layer is formed on a FTO coated glass by a single-step solution spin coating method in the air. We study the effects of different probe materials on the memory cell behavior including silver epoxy, copper and graphite. The device with silver probe shows a bipolar resistive switching behavior with 10^6 on/off resistance ratio in the forming process. The fabricated probe-based memory cell shows a minimum endurance of 10^4 cycles and a minimum retention time of 2×10^3 s. These experimental results confirm that organic-inorganic lead halide perovskite (OILHP) materials are a potential candidate to be used as a storage medium for probe based storage memories. This study provides a better understanding of resistive switching mechanism in organic-inorganic lead halide perovskites thin films that can be useful for understanding of the future probe-based beyond Moore's law memory devices.

1. Introduction

Today, the demand for high capacity data storage devices is growing continuously. The mainstream technologies for massive data storage are hard disks, optical discs and flash memories. The conventional way to increase the memory cell's density is scaling. But all technologies mentioned, face physical limits for being scaled down, e.g. flash memory cells keep information as trapped electric charges on a floating gate and further scaling leads to less stored charges and a bigger leakage current which result in degradation of the memory cells [1]. Another bottleneck to conventional high density memory production is photolithography process which limits the cell scaling due to different constrains in the optical system, resist development, etc. In order to overcome such constraints, probe-based storage memories as a beyond Moore's law memory solution have been proposed. The well-known probe-based technologies include thermo-mechanical probe memories, magnetic probe memories, ferroelectric probe memories and phase-change probe memories. In these memory technologies, information is stored in a storage medium by an external extinction caused by a nanoscale cantilever probe [2].

RRAM is a type of non-volatile memory that stores information as two levels of resistance states [3]. A variety of materials can be used as insulator in metal-insulator-metal (MIM) structure of RRAM cells. Some of these materials include metal oxides [4], inorganic perovskites [5] and graphene oxide [6].

Organic-inorganic lead halide perovskites (OILHP) with its special optical and electrical properties have found a wide range of applications. Beside its photovoltaic applications, OILHP has been used as an active layer in RRAM cell. Perovskites are a type of crystal materials with brief formula of ABX_3, e.g. $CaTiO_3$, in which A is a larger cation, B is a smaller metal cation and X is an anion [7]. For OILHP, A is $CH_3NH_3^+$, B is Pb^{2+} and X is I^-, Br^-, Cl^- or a mixture of them. Most of the papers on memory application of OILHP were on $CH_3NH_3PbI_3$ and only a few of them have focused on Cl content solution precursor perovskite with $CH_3NH_3PbI_{3-x}Cl_x$ formula. There has been a controversy over the role of Cl in OILHP films. It is confirmed that there is a negligible *Cl* content in the final film after annealing process and Cl atoms are evaporated during the annealing process [8]. However, it is demonstrated that Cl content affects the morphology [9], the carrier diffusion length [10] and the stability [11,12] of the deposited film.

Yoo et al. demonstrated the first resistive switching memory device based on $CH_3NH_3PbI_{3-x}Cl_x$ with the structure of Au/Perovskite/FTO. The device shows repeatable bipolar resistive switching with a small on/off ratio of ~2 [13]. Later, they exchanged Au electrode with Ag

* Corresponding author. Department of Electrical Engineering, Ferdowsi University of Mashhad, 9177948974, Mashhad, Iran.
E-mail address: Joodaki@um.ac.ir (M. Joodaki).

https://doi.org/10.1016/j.orgel.2019.03.019
Received 24 September 2018; Received in revised form 18 February 2019; Accepted 11 March 2019
Available online 15 March 2019
1566-1199/ © 2019 Elsevier B.V. All rights reserved.

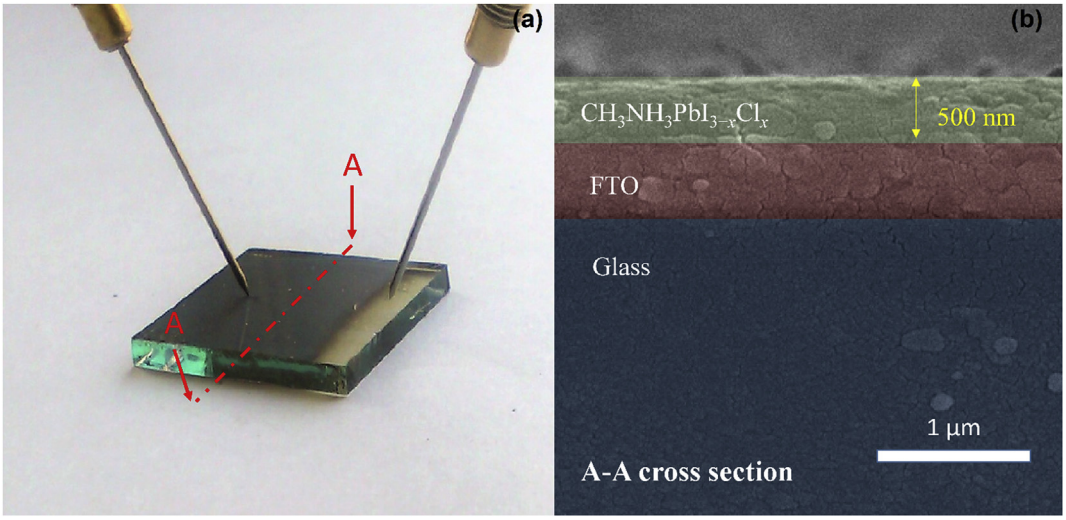

Fig. 1. (a) Test setup used for characterization of the probe-based resistive memory cell. (b) SEM cross section image of $CH_3NH_3PbI_{3-x}Cl_x$ layer formed on FTO/Glass substrate.

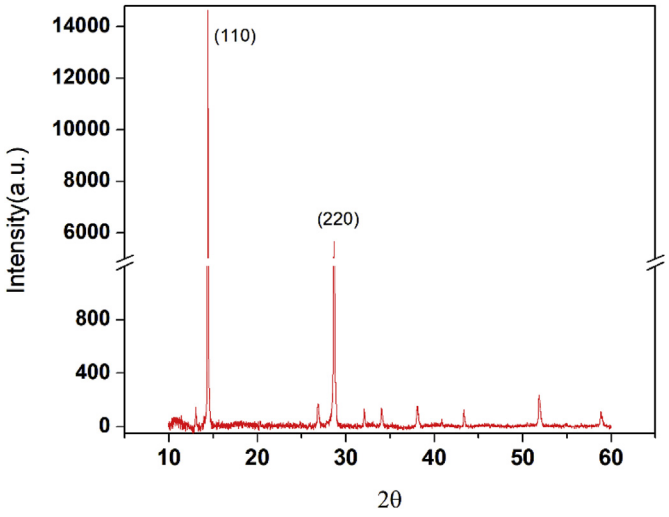

Fig. 2. XRD pattern of the deposited $CH_3NH_3PbI_{3-x}Cl_x$ layer with 500 nm thickness on FTO.

electrode and investigated the dependency of the resistive switching mechanism on the electrode material [14]. Yan et al. fabricated the sandwiched Al/$CH_3NH_3PbI_{3-x}Cl_x$/TiO_2/FTO and achieved the first cycle on/off resistance ratio of 10^9 in lead halide perovskite memories (no endurance test was reported) [15]. They deposited a variety of metals (Au, Ag, Zn, Cu, Ti, Al) as electrode on $CH_3NH_3PbI_{3-x}Cl_x$/FTO structure and they found no significant relationship between the switching voltage and the standard electrode potential of metals. They have also stated that only electrochemically active metals must be used as cation sources for metallic filament built up required for Low resistance states (LRS). Finally, they selected aluminum as the best electrode exhibiting instantaneous switching with a low operating voltage [15]. Yan et al. also demonstrated a fiber–shaped non-volatile memory based on perovskite [16]. The device is fabricated on titanium wire with Ti/TiO_2/$CH_3NH_3PbI_{3-x}Cl_x$/Au structure [16]. The memory cell exhibited an on/off ratio of 20 and a set voltage of 1 V but no data on the endurance performance was reported. After deposition of $CH_3NH_3PbI_{3-x}Cl_x$ on a TiO_2 coated titanium wire, instead of using conventional electrode deposition such as thermal evaporation or sputtering, they entwined the structure with an Au wire to act as the electrode. The Au wire is selected due to its good ductility so that a firm contact formation could be viable. This experiment confirmed that metal-insulator-metal (MIM) memory cells based on OILHP can be fabricated with no use of conventional deposition of electrodes. Recently, an optoelectronic $CH_3NH_3PbI_{3-x}Cl_x$ memory cell on FTO substrate and Au as electrode was introduced by Zhou et al. [17]. The authors studied the effect of light illumination on resistive switching behavior of the cell. They achieved a 0.1 V set voltage for the memory cell under white light illumination with a power density of 3.20 mW cm^{-2}. They observed that the set voltage tended to decrease by increasing the light intensity. Their results paves the way for the application of the perovskite RRAM not only for data storage but also in optical sensing and optical logic devices [17].

Physical mechanisms behind perovskite memristors operation are still under debate and different phenomena have been suggested as the root cause of the resistive switching behavior in perovskite RRAM. It is generally accepted that the defects in OILHP films can be responsible for the memory behavior. In a fresh device before applying an electric field, these defects (e.g. halide vacancies) are evenly distributed all over the perovskite film. However, under the effect of an electrical field, the accumulation and migration of halide vacancies can cause building and rupture of conductive filaments (CFs) leading to a repeatable resistive switching behavior [18–22].

Electrochemical metallization is another mechanism that is believed to cause a resistive switching effect in lead halide perovskite memories. This mechanism depends on metal cation formation of electrochemical active electrodes such as Ag^+ [14,15,23]. The highly mobile metal ions drift to the other electrode and get neutralized by absorbing electrons. This process will be repeated until one or more metal filaments are constructed and the device switches to LRS. Sun et al. fabricated an Ag/$CH_3NH_3PbI_3$/FTO structure to study switching mechanism of lead halide perovskite memories [23]. They showed that the switching mechanism depends on the perovskite thickness. Since formation and migration of Ag^+ ions are only possible at a minimum electric field of $\sim 1 \times 10^7$ V/m, they manifest that Ag filament formation plays a role only in devices with perovskite thicknesses below 90 nm. They concluded that both metal and inherent vacancy CFs are involved in the switching mechanism of lead halide perovskite memristors [23].

The Schottky contact resistance shows a strong dependency on the Schottky barrier height. It is reported that ion migration [24] and charge trapping [17] in perovskite/electrode interface can change the barrier height which, in turn, can lead to a resistive switching effect.

Recently, a conventional resistive memory device based on $CH_3NH_3PbI_3$ with Oleic acid treatment was demonstrated by Cai et al.

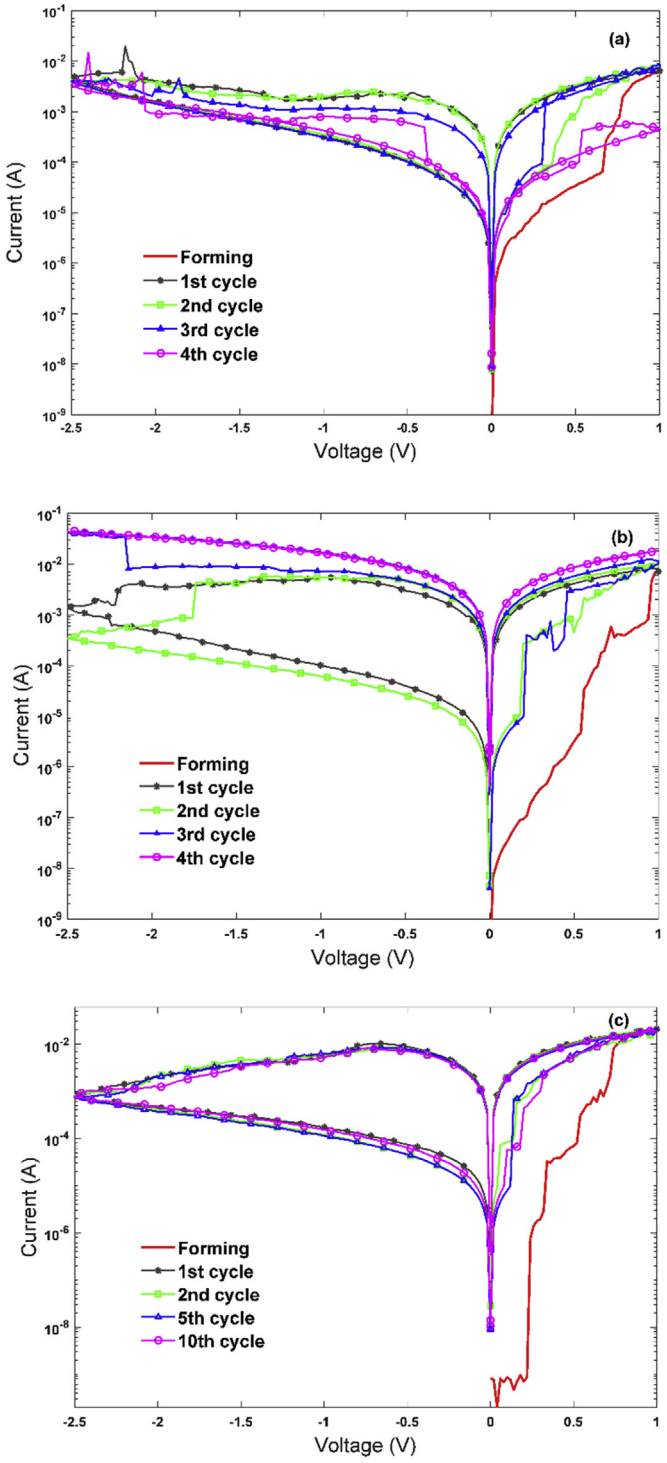

Fig. 3. Measured I-V characteristics of the probe based lead halide perovskite memory cell using different probe materials: (a) Graphite, (b) Cu and (c) Silver epoxy.

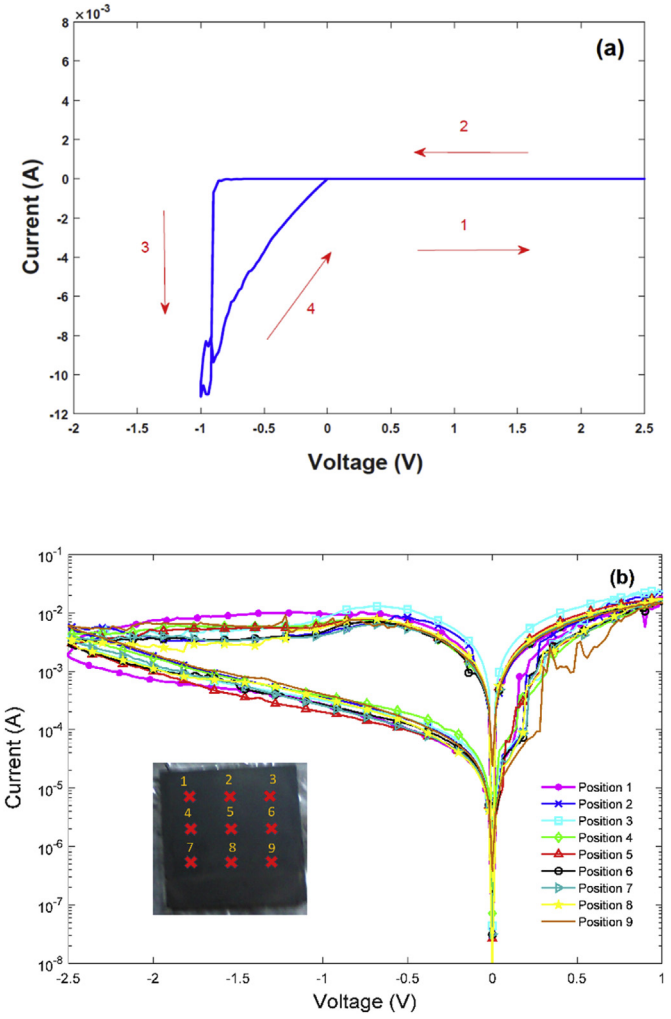

Fig. 4. (a) The measured I-V characteristic of the probe based memory cell with a silver epoxy probe under a reversed voltage sweep. The LRS is not occurred until a positive voltage is applied to the probe needle. (b) I-V characteristics obtained at different locations on the perovskite layer.

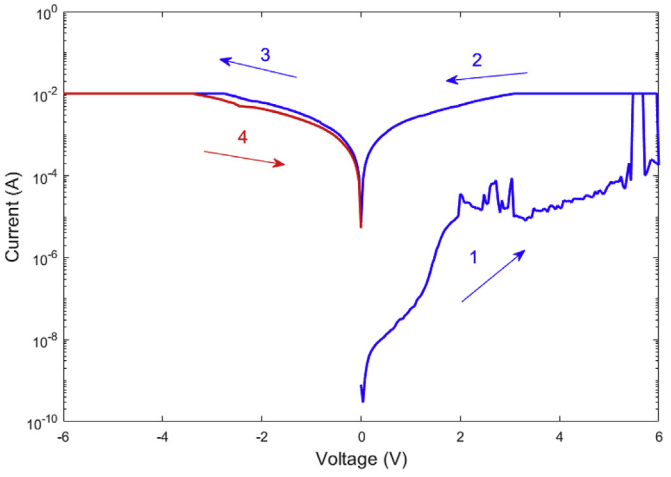

Fig. 5. I-V curve under the voltage sweep of 0 → 6 → 0→ − 6 → 0 measured by the graphite probe tip. The current compliance is set at 10 mA.

[25]. Using the Oleic acid treatment improved the cell behavior and reproducibility. Moreover, they indicated that the passivation process decreases the defect density and this alters the switching mechanism from the ion migration to the barrier modulation mechanism [25].

In this work, we experimentally investigate the probe induced resistive switching in $CH_3NH_3PbI_{3-x}Cl_x$ layer and we also study the effects of different probe materials on the electrical characteristics and reliability parameters of the memory cell. Similar studies on other materials, e.g. SnO_2 layer with a tungsten probe having a tip diameter of 20 μm, have been already reported [26]. We believe this study will highlight the lead halide perovskite as an excellent candidate to be used as a storage medium in probe storage devices.

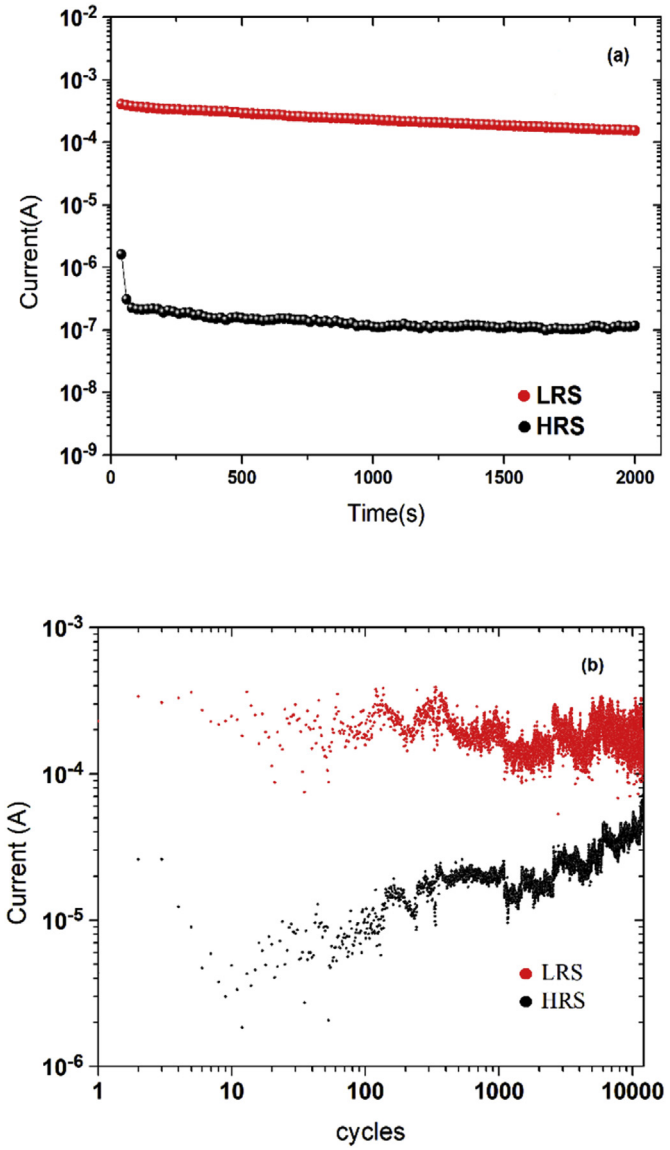

Fig. 6. (a) Data retention time of LRS and HRS states (b) Pulse endurance test result.

2. Experimental section

The perovskite precursor ink was purchased from Ossila Ltd. First the FTO substrate as the bottom electrode was cleaned in deionized water, Acetone, Isopropanol alcohol. After drying the substrate with Argon gas, the $CH_3NH_3PbI_{3-x}Cl_x$ film was deposited by single-step solution spin coating process at 2000 rpm for 30 s followed by a 60 min annealing at 100 °C on a hot-plate. I-V characteristics of the device were measured using a Keithley 2400 semiconductor analyzer. Perovskite layer crystallinity was investigated by XRD experiment using a GNR X-ray explorer with CuKa radiation (λ = 1.5418 Å). Cross-section image of the device were captured by field emission microscopy (MIRA3 TESCAN) with a 15 kV acceleration voltage. All of the device characterization and fabrication steps were performed in the air and under the room temperature.

3. Results and discussion

Fig. 1 shows the test structure and cross sectional view of an SEM image of the perovskite layer with 500 nm thickness deposited on a FTO/glass substrate. In order to check crystallization quality of the

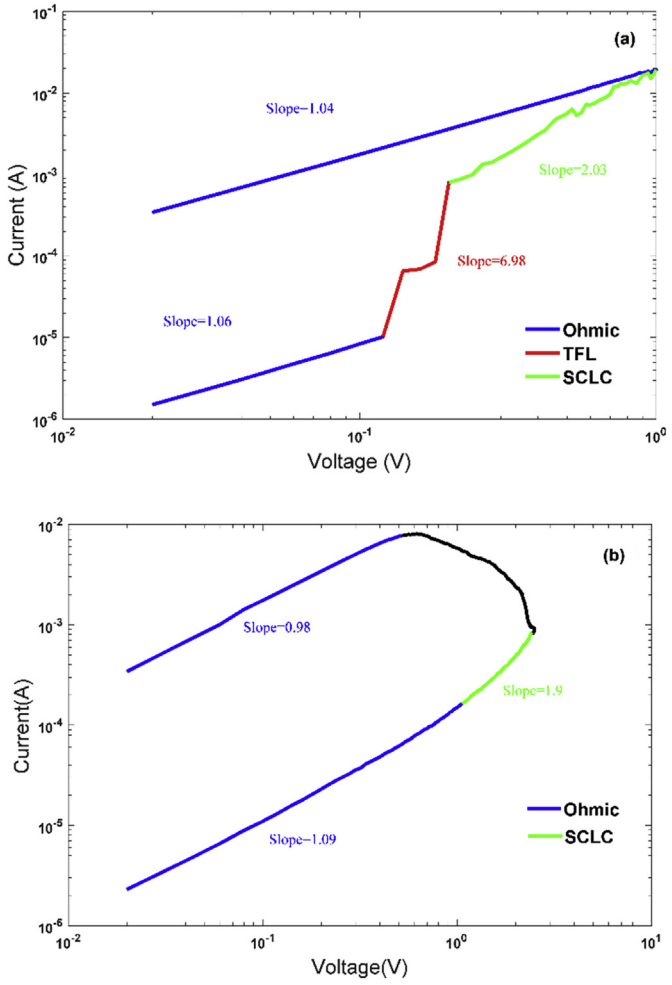

Fig. 7. Plot of Log I -Log V in order to investigate current mechanisms in (a) positive and (b) negative voltage sweep directions.

perovskite thin layer, an X-ray analysis (XRD) was performed, the result of which is presented in Fig. 2. Two intense peaks were observed at $2\theta = 14.4^{\circ}$and $2\theta = 28.8^{\circ}$ corresponding to (110) and (220) crystal lattice planes. This confirms the crystallinity of the deposited perovskite film and shows a good consistency with previously published reports [27].

Silver epoxy, copper and graphite (as a non-metallic probe) were selected in order to investigate the effects of different probe materials on resistive switching behavior of the memory cell. In our experiments, the probes' tip diameter was about 200 μm. Silver and copper as electrode materials have been already used in conventional lead halide perovskite cells and their influences on the memory performance were investigated [14,28] but no information on implementation of carbon allotropes as electrode material for this type of memory cell is found.

The measured current-voltage (I-V) characteristics of the memory cell using different probe materials are given in Fig. 3. As can be seen all three cases show bipolar resistive switching behavior. I-V curves are measured with an applied voltage sweep of 0 V→1 V→0 V→-2.5 V→0 V at a voltage rate of 0.1V/s. Current compliance of 100 mA was set to protect the samples against the electrical overdrive. As shown in Fig. 4(a) positive voltage should be applied to the probe and FTO must be grounded. When a negative voltage is applied to the probe, the device does not switch to the LRS.

The perovskite layer with graphite and copper probes excitations show hysteresis behaviors but as it is shown in Fig. 3 their switching is not repeatable and they show a low endurance cycling. Furthermore, the memory cells characteristics with graphite and copper probes show

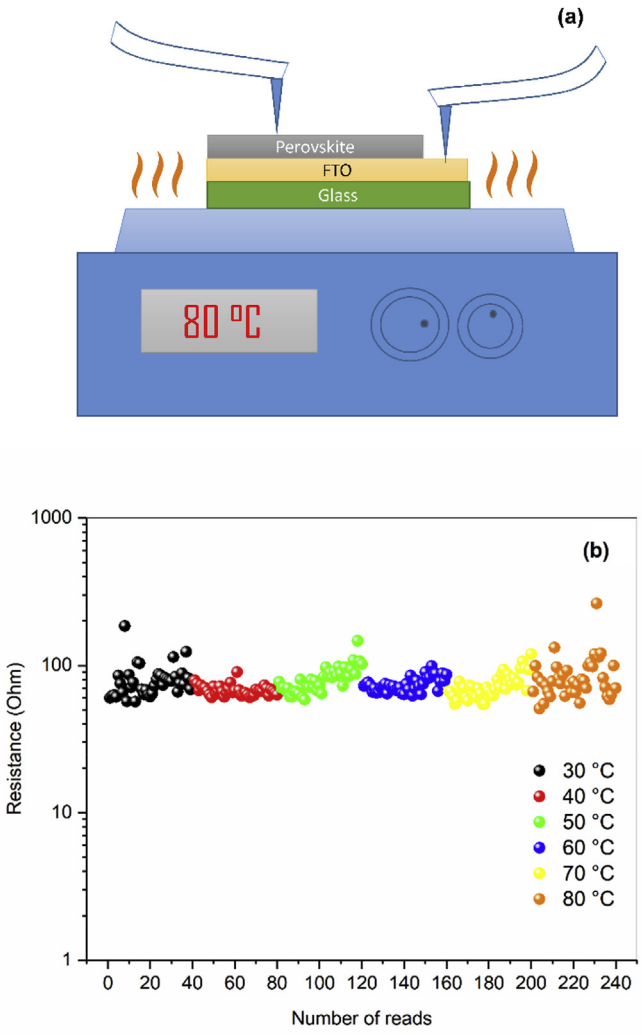

Fig. 8. (a) Test structure used to investigate LRS temperature dependence. (b) Resistance of the LRS in $CH_3NH_3PbI_{3-x}Cl_x$/FTO structure under different temperatures.

a strong dependency on the probe tip position on the perovskite layer. We tried to measure I-V characteristics by using graphite and copper probes at different points on the top surface of the perovskite layer and in most cases no resistive hysteresis behavior was observed even at higher forward voltages and with a current compliance of 10 mA, see Fig. 5. But the probes coated by silver paste, surprisingly showed different results. As shown in Fig. 4(b), impressive uniform resistive switching behavior at different locations on the top surface of the perovskite layer was observed. Therefore, for further investigation, we selected the memory cell with silver epoxy tip due to its uniform response (position independence) and its better endurance performance.

Unlike the majority of the papers published on conventional lead halide perovskite memories, we observed an electroforming process and a higher forming voltage was required to switch on the device in the first voltage sweep. Device shows an on/off ratio of 10^6 in the first cycle. However, after forming process the on/off ratio was reduced to less than 100. The measured LRS and HRS retention times were over $2 \times 10^3 s$ with a reading voltage of 0.02 V at room temperature, see Fig. 6 (a). In order to evaluate the endurance reliability of the device, successive probe-induced read/write operations were performed for 10^4 cycles with a pulse width of 200 ms. The pulse voltage values were 1 V, −2.5 V and 0.02 V for operation sequence of writing, erasing and reading, respectively. The results are presented in Fig. 6(b).

In order to investigate the switching mechanism of the probe-based memory cell, its Log (I) versus Log (V) is plotted in Fig. 7. Space charge limited conduction (SCLC) is a current mechanism that is associated to the traps inside the dielectric layer in MIM structures [29]. The traps are created by defects that a variety of them exist in $CH_3NH_3PbI_{3-x}Cl_x$ films. Fitting the result exhibits three distinct regions as depicted in Fig. 7(a). In the first region at low voltage, only the thermally generated carriers contribute the current. So this region in which the current shows a linear relationship with voltage is called the ohmic region. In the second region, the voltage increases and reaches a value that causes electron injection. As the injected electrons travel across the active layer and reach the counter electrode, the traps inside the dielectric layer start to fill up. This region is called trap field limited region (TFL). SCLC region appears when the occupation of traps inside the film is finished and the space charge is built. The minimum voltage required for this space charge built-up is named trap filled limited voltage (V_{TFL}). The measured V_{TFL} of the device under test was 0.24 V.

If a sufficiently high negative voltage is applied, the memory cell switches to HRS. When the voltage across the device is swept from −2.5 V to 0 V, the current mechanism changes from SCLC to ohmic, see Fig. 7(b).

Theoretical studies show that the iodide vacancies have a low activation energy to migrate among the defects available in OILHD films [18,20]. Experimental observations also report that I/Pb ratio is reduced in the direction of the applied electric field which can be considered as an evidence that the iodide vacancies migration is responsible for resistive switching behavior in lead halide perovskite conventional memories [19,20].

Here, we have investigated the effect of the silver epoxy coated probe on the resistive switching mechanism of lead halide perovskite memories. The electric field required to set our probe based memory cell considering the perovskite layer thickness of 500 nm and the set voltage of 0.24 is 4.8×10^5 V/m, which is two orders of magnitude lower than that of Ag ion formation reported in Ref. [23].

Temperature dependency of LRS is usually considered as an indicator of the formation of metallic filaments [15,23]. In order to investigate the temperature dependency of the LRS, the temperature was increased from 30 °C to 80 °C in six steps, Fig. 8(a). A 5 min pause is made after each step to stabilize the temperature of the sample. Resistance of the LRS was measured 40 times at each step by performing write/read/erase operations sequence. The tip's position was kept fixed during the test. As it is well demonstrated in Fig. 8(b) the measured LRS shows no temperature dependency. In LRS, the resistance of our device in most of cycles changes from 60 Ω to 80 Ω due to the random variations in dimensions of the CFs which leads to an average value of about 70 Ω. Here, as the range of resistance fluctuations with temperature is less than those of related to the dimension variations of the CFs during successive write/erase operations, the resulted LRS resistance is not strongly affected by temperature. In lead halide perovskite materials, iodide vacancies can act as donors and accumulation of iodide vacancies can lead to formation of highly conductive filaments [20]. Therefore, based on our device mechanism of current, ion migration and charge trapping can lead to formation of CFs and Fermi level pinning near the conduction band. So, the fixed Fermi level can be responsible for the temperature independency observed here. This is in opposite to the strong temperature dependency of perovskite memory cell with silver CFs and 90 Ω cell resistance reported in Ref. [23]. Furthermore, hysteresis in I-V measurement of memory cells with non-metallic probe was also observed, see Fig. 3(a).

So these results suggest that no electrochemical activity of the metal probe can play a notable role in the resistive switching mechanism of the device and the memory behavior of the cell with silver epoxy coated probe can be related to the formation of an electrically conductive path by the accumulation of inherent perovskite defects. In this work, different probe tips are used on the surface of the perovskite layer to program the cell directly. An important issue that must be considered here is the probe tip specifications such as probe material, probe radii,

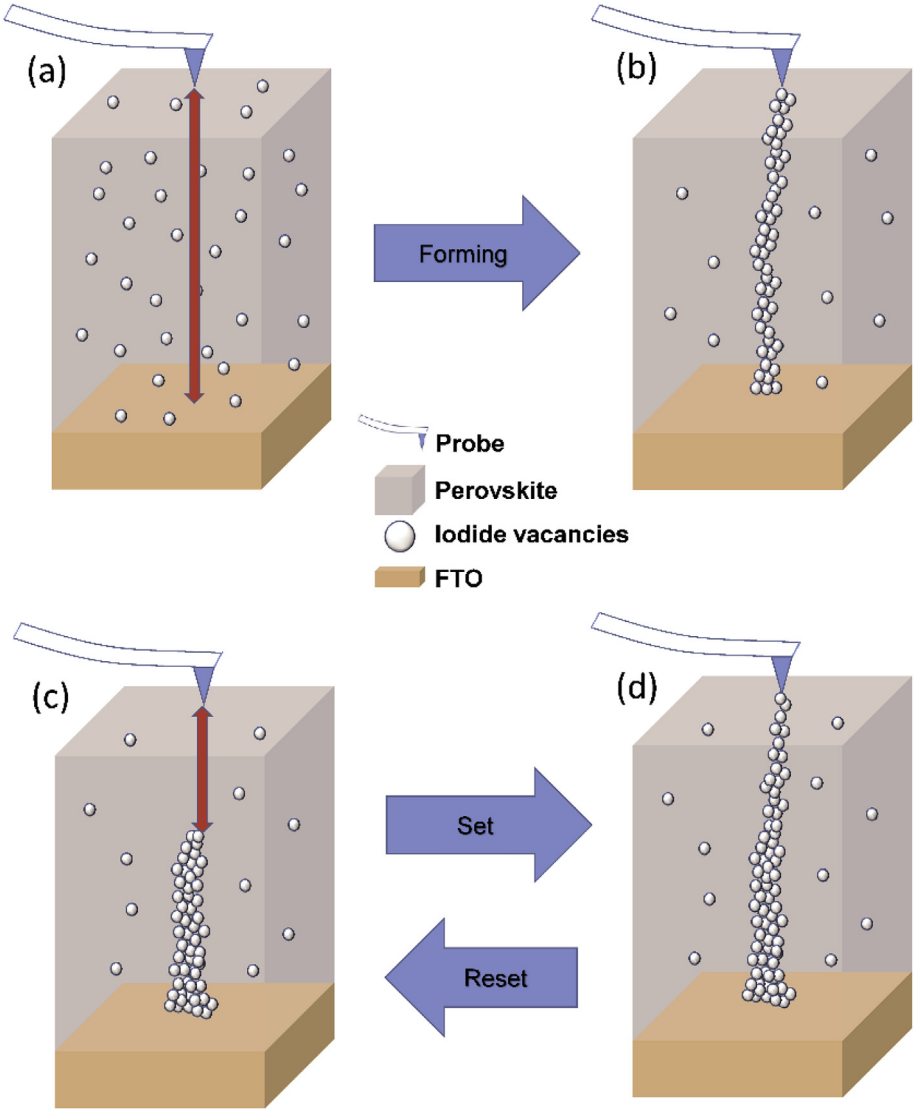

Fig. 9. Graphical illustration for resistive switching mechanism of device. (a) Original state of device. (b) Filament construction after forming process. (c) Off state and (d) On state of device.

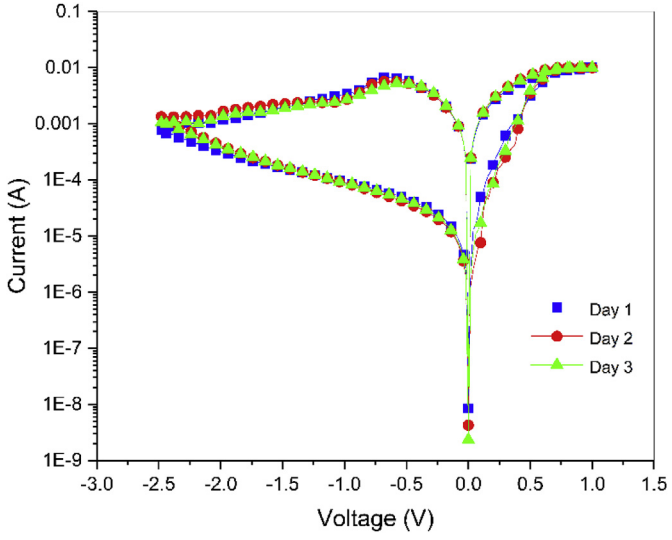

Fig. 10. I-V characteristics of $CH_3NH_3PbI_{3-x}Cl_x$/FTO was measured in 3 days. The device was kept in the air without any protection.

probe softness and applied pressure. Thus, different probe tip specifications lead to different types of contact formation showing different behaviors. The impressive memory performance observed with the silver probe is possibly related to its proper mechanical specifications that result in a better electrical contact formation.

As shown in Fig. 4(a), the device switches to LRS only by applying a positive voltage to the perovskite layer. This may be considered as an evidence for positive metal ion migration through the perovskite layer in the direction of the applied electric field. However, according to our best knowledge, there is no report on vertical MIM memory cell structures with inert metal electrodes which can switch to LRS by applying a voltage with different polarities. This phenomenon could be related to different charge injection characteristics at different electrodes, however this effect is not yet well explained in the literature and requires further investigations.

In the fresh device (before applying any voltage), the iodide vacancies are distributed evenly over the perovskite film and a maximum gap exists between the probe and FTO electrode as indicated with a red arrow in Fig. 9(a). Therefore, a high voltage is needed to set the cell (forming process). If a positive voltage is applied, iodide vacancies with positive charge migrate toward the FTO layer, as the cathode, and accumulate until CFs are constructed and the device switches to LRS. In

the reset process, when a negative voltage is applied, negatively charged iodide ions which are accumulated near the anode start to fill up the vacancies and repute the CFs. As the current path is destructed, all the voltage applied by the probe drops across the small gap which is shown as a red arrow in Fig. 9(c). Therefore, the device never comes back to its original state prior to the forming process. As a result, the smaller on/off resistive ratio is associated to partial CFs destruction. A part of the conductive path which is not destructed in set and reset operations, get thicker and the gap becomes smaller resulting in smaller HRS and on/off resistive ratio as can be seen from the endurance test result, see Fig. 6(b).

A major problem of lead halide perovskites is their instability against oxygen and humidity. Since no top-electrode is used in our structure and the device is in direct contact with the air, we investigated the stability of device and the results are given in Fig. 10. These I-V characteristics were measured at room temperature with no protections against the air. The measurements were repeated each 24 h at 10 different points on the top surface of the perovskite layer. The average value of the 10 measured currents for each day is plotted in Fig. 10. The stability performance observed here is comparable with that of the conventional memory cells with top electrode reported in Ref. [30]. It goes without saying, adding a passivation layer [30] or applying suitable packaging may improve the stability of the device.

In probe-based memory technologies the size of the cell is primary determined by the diameter of the tip. In filamentary switching mechanisms, the minimum cell size is determined by the nanoscale conductive filament. This can result in a highly scalable memory technology. So, combining the advantages of the probe-based memories with the scalability of the filamentary switching memories can pave the way for design and development of high density memories. Although the 3D integration of conventional RRAM cell is another approach to increase the memory density, it suffers from several restrictions especially at nanoscale dimensions such as sneak current, high wire resistance, high parasitic capacitors and high current density affordable by the selectors and metal lines [31]. Further studies, especially with nanoscale probes, are needed for a real evaluation of the practical application of this type of memory.

Recently, Rangelow et al. demonstrated AFM integrated with an SEM microscope system which was designed and developed for atomic-scale device fabrication and characterization [32,33]. By using this system, they investigated the effects of tip shape, tip material, applied voltage and the tip distance on the field emission current on the tip. In order to investigate the effect of the tip's material on the field emission current, they fabricated and tested different nanoscale tips based on silicon, GaN, diamond, and tungsten [34]. So we believe, doing similar studies on our memory cell can provide valuable information about the performance and limitations of this device. For example, there are several important questions that must be answered including what is the minimum cell size in this technology, what are the nanoscale tip's properties effects on the memory cell behavior or which tip's material or which type of the active layer gives the best memory performance.

4. Conclusion and future prospects

In summary, in this work we achieved a resistive switching memory without deposition of any metal as the top electrode. The resistive switching was induced by a probe voltage applying to $CH_3NH_3PbI_{3-x}Cl_x$ film. We investigated the effect of the probe materials of graphite, copper and silver paste on resistive switching behavior. This approach helps us investigate resistive switching behavior of individual perovskite thin film without the effect of top electrode. Our results demonstrated that the resistive switching of the device is based on CFs construction resulting from inherent perovskite defect accumulation between the probe and FTO electrode. Our study in this paper helps to gain insight into migration and redistribution of the defects in OILHP thin films under probe excitation. This is a significant step toward understanding and development of this type of memories. Though a reliable memory behavior was observed for the silver epoxy coated probe, further studies, especially with nanoscale tips, are needed for a fair evaluation of the memory cell, which can be used as a beyond Moore probe based on non-volatile resistive memory. A major topic for future study can be the scaling of such cells and achieving uniform memory characteristics over the entire memory array with nanoscale dimensions.

Acknowledgements

This work was supported by the Ferdowsi University of Mashhad, Mashhad, Iran under Grant No. of 46946.

References

[1] M. Joodaki, Uprising nano memories: latest advances in monolithic three dimensional (3D) integrated Flash memories, Microelectron. Eng. 164 (2016) 75–87.
[2] L. Wang, C.H. Yang, J. Wen, S. Di Gong, Y.X. Peng, Overview of probe-based storage technologies, Nanoscale research letters 11 (2016) 342.
[3] M. Joodaki, Selected Advances in Nanoelectronic Devices: Logic, Memory and RF, Springer, 2013.
[4] D. Ielmini, Resistive switching memories based on metal oxides: mechanisms, reliability and scaling, Semicond. Sci. Technol. 31 (2016) 063002.
[5] Z. Yan, J.-M. Liu, Resistance switching memory in perovskite oxides, Ann. Phys. 358 (2015) 206–224.
[6] C. He, F. Zhuge, X. Zhou, M. Li, G. Zhou, Y. Liu, J. Wang, B. Chen, W. Su, Z. Liu, Nonvolatile resistive switching in graphene oxide thin films, Appl. Phys. Lett. 95 (2009) 232101.
[7] R.E. Schaak, T.E. Mallouk, Perovskites by design: a toolbox of solid-state reactions, Chem. Mater. 14 (2002) 1455–1471.
[8] H. Yu, F. Wang, F. Xie, W. Li, J. Chen, N. Zhao, The role of chlorine in the formation process of "$CH_3NH_3PbI_{3-x}Cl_x$" perovskite, Adv. Funct. Mater. 24 (2014) 7102–7108.
[9] S.T. Williams, F. Zuo, C.-C. Chueh, C.-Y. Liao, P.-W. Liang, A.K.-Y. Jen, Role of chloride in the morphological evolution of organo-lead halide perovskite thin films, ACS Nano 8 (2014) 10640–10654.
[10] S.D. Stranks, G.E. Eperon, G. Grancini, C. Menelaou, M.J. Alcocer, T. Leijtens, L.M. Herz, A. Petrozza, H.J. Snaith, Electron-hole diffusion lengths exceeding 1 micrometer in an organometal trihalide perovskite absorber, Science 342 (2013) 341–344.
[11] Y. Chen, T. Chen, L. Dai, Layer-by-Layer growth of $CH_3NH_3PbI_{3-x}Cl_x$ for highly efficient planar heterojunction perovskite solar cells, Adv. Mater. 27 (2015) 1053–1059.
[12] J. Chae, Q. Dong, J. Huang, A. Centrone, Chloride incorporation process in $CH_3NH_3PbI_{3-x}Cl_x$ perovskites via nanoscale bandgap maps, Nano Lett. 15 (2015) 8114–8121.
[13] E.J. Yoo, M. Lyu, J.H. Yun, C.J. Kang, Y.J. Choi, L. Wang, Resistive switching behavior in organic–inorganic hybrid $CH_3NH_3PbI_{3-x}Cl_x$ perovskite for resistive random access memory devices, Adv. Mater. 27 (2015) 6170–6175.
[14] E. Yoo, M. Lyu, J.-H. Yun, C. Kang, Y. Choi, L. Wang, Bifunctional resistive switching behavior in an organolead halide perovskite based Ag/CH 3 NH 3 PbI 3 − x Cl x/FTO structure, J. Mater. Chem. C 4 (2016) 7824–7830.
[15] K. Yan, M. Peng, X. Yu, X. Cai, S. Chen, H. Hu, B. Chen, X. Gao, B. Dong, D. Zou, High-performance perovskite memristor based on methyl ammonium lead halides, J. Mater. Chem. C 4 (2016) 1375–1381.
[16] K. Yan, B. Chen, H. Hu, S. Chen, B. Dong, X. Gao, X. Xiao, J. Zhou, D. Zou, First fiber-shaped non-volatile memory device based on hybrid organic–inorganic perovskite, Advanced Electronic Materials 2 (2016).
[17] F. Zhou, Y. Liu, X. Shen, M. Wang, F. Yuan, Y. Chai, Low-voltage, optoelectronic $CH_3NH_3PbI_{3-x}Cl_x$ memory with integrated sensing and logic operations, Adv. Funct. Mater. 28 (2018) 1800080.
[18] C. Gu, J.-S. Lee, Flexible hybrid organic–inorganic perovskite memory, ACS Nano 10 (2016) 5413–5418.
[19] D.J. Kim, Y.J. Tak, W.G. Kim, J.K. Kim, J.H. Kim, H.J. Kim, Resistive switching properties through iodine migrations of a hybrid perovskite insulating layer, Advanced Materials Interfaces 4 (2017).
[20] X. Zhu, J. Lee, W.D. Lu, Iodine vacancy redistribution in organic–inorganic halide perovskite films and resistive switching effects, Adv. Mater. (2017) 29.
[21] G. Landi, V. Subbiah, K.S. Reddy, A. Sorrentino, A. Sambandam, P.C. Ramamurthy, H.-C. Neitzert, Evidence of bipolar resistive switching memory in perovskite solar cell, IEEE Journal of the Electron Devices Society 6 (2018) 454–463.
[22] J. Choi, S. Park, J. Lee, K. Hong, D.H. Kim, C.W. Moon, G.D. Park, J. Suh, J. Hwang, S.Y. Kim, Organolead halide perovskites for low operating voltage multilevel resistive switching, Adv. Mater. 28 (2016) 6562–6567.
[23] Y. Sun, M. Tai, C. Song, Z. Wang, J. Yin, F. Li, H. Wu, F. Zeng, H. Lin, F. Pan, Competition between metallic and vacancy defect conductive filaments in a $CH_3NH_3PbI_3$-based memory device, J. Phys. Chem. C 122 (2018) 6431–6436.
[24] X. Guan, W. Hu, M.A. Haque, N. Wei, Z. Liu, A. Chen, T. Wu, Light-responsive ion-redistribution-induced resistive switching in hybrid perovskite Schottky junctions, Adv. Funct. Mater. 28 (2018) 1704665.
[25] H. Cai, G. Ma, Y. He, C. Liu, H. Wang, A remarkable performance of $CH_3NH_3PbI_3$

perovskite memory based on passivated method, Org. Electron. 58 (2018) 301–305.
[26] C.-C. Hsu, P.-Y. Chuang, Y.-T. Chen, Resistive switching characteristic of low-temperature top-electrode-free tin-oxide memristor, IEEE Trans. Electron Devices 64 (2017) 3951–3954.
[27] X. Yan, W. Wang, X. Yang, W. Yi, Y. Wang, H. Li, W. Gu, C. Sheng, Origin of thermal instability of $CH_3NH_3PbI_{3-x}Cl_x$ films for photovoltaic devices, Mater. Lett. 176 (2016) 114–117.
[28] G. Lin, Y. Lin, R. Cui, H. Huang, X. Guo, C. Li, J. Dong, X. Guo, B. Sun, An organic–inorganic hybrid perovskite logic gate for better computing, J. Mater. Chem. C 3 (2015) 10793–10798.
[29] F.-C. Chiu, A review on conduction mechanisms in dielectric films, Advances in Materials Science and Engineering (2014) s.
[30] B. Hwang, J.S. Lee, Hybrid organic-inorganic perovskite memory with long-term stability in air, Sci. Rep. 7 (2017) 1–7, https://doi.org/10.1038/s41598-017-00778-5.
[31] J.Y. Seok, S.J. Song, J.H. Yoon, K.J. Yoon, T.H. Park, D.E. Kwon, H. Lim, G.H. Kim, D.S. Jeong, C.S. Hwang, A review of three-dimensional resistive switching cross-bar array memories from the integration and materials property points of view, Adv. Funct. Mater. 24 (2014) 5316–5339, https://doi.org/10.1002/adfm.201303520.
[32] I.W. Rangelow, M. Kaestner, T. Ivanov, A. Ahmad, S. Lenk, C. Lenk, E. Guliyev, A. Reum, M. Hofmann, C. Reuter, M. Holz, Atomic force microscope integrated with a scanning electron microscope for correlative nanofabrication and microscopy, J. Vac. Sci. Technol. B 36 (2018), https://doi.org/10.1116/1.5048524 06J102.
[33] M. Holz, E. Guliyev, A. Ahmad, T. Ivanov, A. Reum, M. Hofmann, C. Lenk, M. Kaestner, C. Reuter, S. Lenk, I.W. Rangelow, N. Nikolov, Field-emission scanning probe lithography tool for 150 mm wafer, J. Vac. Sci. Technol. B 36 (2018), https://doi.org/10.1116/1.5048357 06JL06.
[34] C. Lenk, S. Lenk, M. Holz, E. Guliyev, M. Hofmann, T. Ivanov, I.W. Rangelow, M. Behzadirad, A.K. Rishinaramangalam, D. Feezell, T. Busani, Experimental study of field emission from ultrasharp silicon, diamond, GaN, and tungsten tips in close proximity to the counter electrode, J. Vac. Sci. Technol. B 36 (2018), https://doi.org/10.1116/1.5048518 06JL03.